

Beam splitter for spin waves in quantum spin network

S. Yang¹, Z. Song^{1,a}, and C.P. Sun^{1,2,b}

¹ Department of Physics, Nankai University - Tianjin 300071, P.R. China

² Institute of Theoretical Physics, Chinese Academy of Sciences - Beijing 100080, P.R. China

Received 26 February 2006 / Received in final form 2 June 2006

Published online 7 August 2006 – © EDP Sciences, Società Italiana di Fisica, Springer-Verlag 2006

Abstract. We theoretically design and analytically study a controllable beam splitter for the spin wave propagating in a star-shaped (e.g., a Y-shaped beam) spin network. Such a solid state beam splitter can display quantum interference and quantum entanglement by the well-aimed controls of interaction on nodes. It will enable an elementary interferometric device for scalable quantum information processing based on the solid system.

PACS. 03.65.Ud Entanglement and quantum nonlocality – 75.10.Jm Quantized spin models – 03.67.Lx Quantum computation

1 Introduction

Beam splitters are the elementary optical devices frequently used in classical and quantum optics [1], which can even work well in the level of single photon quanta [2] and are applied to generate quantum entanglement [3]. For matter waves, an early beam splitter can be referred to the experiments of neutron interference based on a perfect crystal interferometer with wavefront and amplitude division [4]; and now an atomic beam splitter has been experimentally implemented on the atom chip [5]. The theoretical protocols have been suggested to realize the beam splitter for the Bose-Einstein condensate [6].

In this paper, we propose and study the implementation of beam splitter for the spin wave propagations in the star-shaped spin networks (SSSNs) with $m + 1$ weighted legs (see Fig. 1a), where each leg is a one-dimensional (1-D) spin chain with XY couplings. This investigation is mostly motivated by the recent researches on the perfect transfer of quantum states along a single quantum spin chain [7–9] and for a 1-D Bloch electron system [10,11]. The similar shape quantum networks have been considered for the coupled harmonic oscillators system [12], the spin networks with deliberated engineered couplings [13], quantum cloning via spin networks [14,15], and quantum algorithm [16].

A basic SSSN is a Y-shaped network or called Y-beam [5] for $m = 2$, which can be regarded as an elementary block, in principle, to the architecture of complicated networks (such as a solid state interferometer) for quantum information processing. It can function to

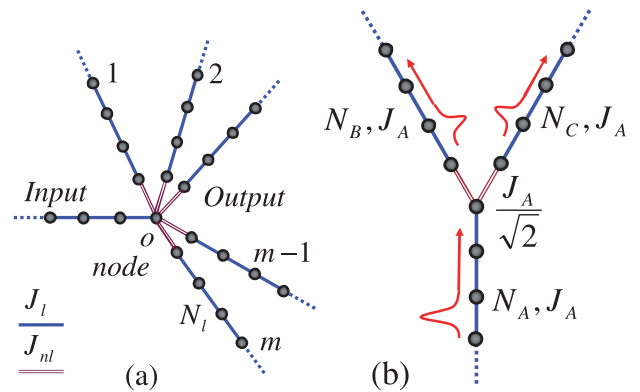


Fig. 1. (Color on line) (a) The star-shaped spin network with an input spin chain A and m output spin chain. (b) Y-shaped network or called Y-beam, a special star-shaped spin network, serves as the fundamental block for the architecture of complicated quantum spin networks.

transfer quantum state coherently in multi-channel and to generate entanglement between two spins which are a long distance apart. Furthermore, we will show that the quantum coherence of spin waves propagating in two legs can be well controlled by adjusting the coupling strengths only at the node; and then a controllable solid state interferometer is built based on this crucial function. The basic element of an arbitrary spin network is the coupling between spins, which is usually described by the XY Hamiltonian as

$$H^{XY} = \sum_{\langle ij \rangle} (J_{ij} S_i^+ S_j^- + H.c.), \quad (1)$$

^a e-mail: songtc@nankai.edu.cn

^b e-mail: suncp@itp.ac.cn

where S_i^\pm are the Pauli spin operators acting on the internal space of electron on the i th site. The sum is assumed to be over nearest neighbors hereafter. One can apply magnetic field B_z beforehand and then switch off it, to prepare a polarized initial states with all spins down for the quantum network. The dynamics of the lower excitations (magnons) from this polarized state is attractive because of their relevance to quantum information applications [7]. In the low-temperature and low magnon density limit, the magnon can be regarded as boson by the Holstein-Primakoff transformation $S_j^+ \simeq b_j^\dagger$ [17]. As to our paper, we only consider the single magnon case. Then one can translates a XY spin network into the bosonic system with the Hamiltonian $b_j^\dagger b_{j+1} + h.c.$, approximately.

2 Star-shaped beam splitter and its reduction

We consider a spin network of a star shape (we call the SSSN) as shown in Figure 1a. Under the Holstein-Primakoff transformation the Hamiltonian of leg l consisting of N_l spins with XY interactions can be written as

$$H_l = H_l(J_l, N_l) = J_l \sum_{j=1}^{N_l-1} (b_{l,j}^\dagger b_{l,j+1} + H.c.), \quad (2)$$

where $b_{l,j}^\dagger, b_{l,j}$ are the boson operators on the j th site of the l th leg. Here we have assumed that the couplings J_l are the same for a given bosonic chain l . We uniquely denote the Hamiltonian by $H_l(J_l, N_l)$ for the bosonic chain hereafter. The SSSN is constructed by linking the m output bosonic chains to the one end (or the node) O of the input leg A by the couplings J_{nl} . The Hamiltonian of an SSSN is of the form as the same as equation (2) except for the part around the node O .

We will show that, due to the quantum interference mechanism, by some constrain for the coupling constants J_l and J_{nl} , an SSSN can be reduced into m independent imaginary linear bosonic chains with homogeneous couplings, one of which has the length equals to the total length of the input leg and the output leg, while the rest $m-1$ chains have the length equal to the ones of the output leg if only the single-magnon case is concerned. The fact that the input chain A is a part of this virtual linear chain implies that the bosonic wave packet can perfectly propagate in this virtual linear chain without the reflection by the node. This indicates that there is a coherent split of the input bosonic wave packet because the magnon excitation in this virtual chain actually is just a superposition of magnon excitations in the m bosonic chains.

To sketch the central idea, we first consider a general SSSN, which consists of m identical ‘‘output’’ chains B_1, B_2, \dots, B_m with homogeneous coupling $J_l = J$, $J_{nl} = J_n$ and the same length N , while the length of chain A is M . The Hamiltonian

$$H = \sum_{p=1}^m H_{B_p}(J, N) + H_A(J, M) + H_{nod} \quad (3)$$

can be explicitly written in terms of the leg Hamiltonians $H_{B_p}(J, N)$ and $H_A(J, M)$ defined by equation (1) and the interactions around the node O

$$H_{nod} = -(b_{A,M}^\dagger \sum_{p=1}^m J_{nB_p} b_{B_p,1} + H.c.). \quad (4)$$

Now we construct the virtual bosonic chain a of length $M+N$ with the boson operators $b_{a,j}^\dagger = b_{A,j}^\dagger$ ($j = 1, 2, \dots, M$) in the real chain A and the collective operator $b_{a,M+j}^\dagger = (1/\sqrt{m}) \sum_{p=1}^m b_{B_p,j}^\dagger$ for the virtual part, where $j = 1, 2, \dots, N$. There exist $m-1$ complementary linear bosonic chains with the collective operators

$$b_{b_q,j}^\dagger = (1/\sqrt{m}) \sum_{p=1}^m \exp(-i2\pi pq/m) b_{B_p,j}^\dagger \quad (5)$$

where $q = 1, 2, \dots, m-1$. It can be checked that, together with $b_{a,j}^\dagger$, the above defined collective operators $b_{a,M+j}^\dagger$ and $b_{b_q,j}^\dagger$, ($q = 1, 2, \dots, m-1$) and their conjugates also satisfy the commutative relations of boson operators.

Using operators $b_{a,M+j}^\dagger$ and $b_{b_q,j}^\dagger$, we divide the total Hamiltonian into two commutative parts

$$H_b = \sum_{q=1}^{m-1} H_{b_q}(J, N); H_a = H_a(J, M+N) + H_{vn},$$

$$H_{vn} = (J - \sqrt{m}J_n) b_{a,M}^\dagger b_{a,M+1} + H.c. \quad (6)$$

The first Hamiltonian H_b describes $m-1$ independent virtual bosonic chains without input from H_A while the second one describes a linear bosonic chain with an impurity at the M th site. Usually, it can reflect the bosonic wave packet from the input leg.

Only when the coupling matching condition $J_n = J/\sqrt{m}$ is satisfied, the virtual bosonic chain described by H_a is just a standard bosonic chain since $H_{vn} = 0$. In this case no reflection occurs at the node. With this matched node coupling, an ideal beam splitter can be realized with m coherent outputs since each operator $b_{a,M+j}^\dagger$ is a linear combination of $b_{B_p,j}^\dagger$. Then it can create a superposition from the vacuum state with bosons excitation. Each component of this superposition represents a magnon or boson excitation in a leg. Actually, the SSSN can be extended to a more general case with different J_{nB_p} ($p = 1, 2, \dots, m$). For an arbitrary set of J_{nB_p} , we introduce the collective operators as

$$b_{a,M+j}^\dagger = \sum_{p=1}^m u_{B_p,a} b_{B_p,j}^\dagger = \sum_{p=1}^m \frac{J_{nB_p}^*}{\sqrt{\sum_{p=1}^m |J_{nB_p}|^2}} b_{B_p,j}^\dagger$$

$$b_{b_q,j}^\dagger = \sum_{p=1}^m u_{B_p,b_q} b_{B_p,j}^\dagger \quad (7)$$

where $u_{B_p,G}$ ($p = 1, 2, \dots, m, G = a, b_1, b_2, \dots, b_{m-1}$) compose a unitary matrix U . Therefore, the above corrective

operators and their conjugates also satisfy the commutative relations of boson operators. In addition, when the general constrain condition $\sum_{p=1}^m |J_{nB_p}|^2 = J^2$ is satisfied, the SSSN can be completely reduced to a virtual homogeneous bosonic chain with $M + N$ sites and $m - 1$ independent virtual bosonic chains. Interestingly, the values of J_{nB_p} can determine the amplitudes of the bosonic wave packet on leg B_p . The detailed analysis will be done with the special SSSN of $m = 2$ in the next section.

3 Y-shaped beam splitter decoupling

To be convenient, we consider the asymmetric Y -beam consisting of three legs A , B and C with three hopping integrals J_F for $F = A, B, C$ and the node interactions J_{nF} for $F = B, C$, see also fig. 1b. The total Hamiltonian reads

$$H = \sum_{F=A,B,C} H_F - \sum_{F=B,C} (J_{nF} b_{A,M}^\dagger b_{F,1} + H.c.) \quad (8)$$

where $H_F = H_F(J_F, N_F)$ and $N_A = M$, $N_B = N_C = N$.

In order to decouple this Y -beam as two virtual linear bosonic chains, we need to optimize the asymmetric couplings so that the perfect transmission can occur in the decoupled linear bosonic chains. To this end we introduce two sets of operators by

$$\begin{aligned} b_{a,M+j}^\dagger &= \cos \theta b_{B,j}^\dagger + \sin \theta b_{C,j}^\dagger; \\ b_{b,j}^\dagger &= \sin \theta b_{B,j}^\dagger - \cos \theta b_{C,j}^\dagger, \end{aligned} \quad (9)$$

for $j = 1, 2, \dots, N$. A straight forward calculation shows that the two sets of operator act as boson operators and commutative. Here, the mixing angle θ is to be determined as follows by the optimization for quantum information transmission. In comparison with the optical beam splitter, the above equation can be regarded as a fundamental issue for the boson beam splitter.

Together with the original boson operator $b_{a,j}^\dagger = b_{A,j}^\dagger$ for the input leg, the set with $b_{a,M+j}^\dagger$ defines a new linear chain a with the effective couplings $J_{aj} = J_A$ ($j \in [1, M - 1]$), $J_{aM} = J_{nB} \cos \theta + J_{nC} \sin \theta$ and $J_{a,M+j} = J_B \cos^2 \theta + J_C \sin^2 \theta$, for $j \in [1, N - 1]$. Another virtual linear chain b is defined by $b_{b,j}^\dagger$ with homogeneous couplings $J_{bj} = J_B \sin^2 \theta + J_C \cos^2 \theta$ for $j \in [1, N - 1]$.

In general, these two linear chains do not decouple with each other since there exists a connection interaction

$$\begin{aligned} H_{con} = g \sum_{j=1}^{N-1} (b_{b,j}^\dagger b_{a,M+j+1} + b_{a,M+j}^\dagger b_{b,j+1} + H.c.) \\ - J_{AB} (b_{a,M}^\dagger b_{b,1} + H.c.) \end{aligned} \quad (10)$$

where $g = (J_B - J_C) \sin 2\theta/2$ and $J_{AB} = J_{nB} \sin \theta - J_{nC} \cos \theta$. Fortunately, the two bosonic chains decouple with each other when we optimize the mixing angle θ and the inter-chain coupling by setting them as

$\tan \theta = J_{nC}/J_{nB}$, $J_B = J_C$ and then $J_{aM} = J_{nB}/\cos \theta$. Thus when we set $J_{nB} = J_A \cos \theta$, the coupling matching condition

$$J_A = \sqrt{J_{nC}^2 + J_{nB}^2} = J_B = J_C \quad (11)$$

holds. Here, J_{nB} and J_{nC} can be real or complex, which will not affect the final results. Especially, the virtual bosonic chain a becomes homogenous when condition (11) is satisfied. Then it can be employed to transfer the quantum state without reflection on the node in the transformed picture. By transforming back to the original picture, the quantum state transfer is shown to be a perfect beam splitting. Similar to the point of view of linear optics, such beam splitting process can generate entanglement. We will show that the magnitudes of J_{nB} and J_{nC} can determine the amplitudes of the bosonic wave packet on legs B and C .

Now we apply the beam splitter to a special spin wave packet, a Gaussian wave packet (GWP) with momentum $\pi/2$, which has the form

$$|\psi_{A\frac{\pi}{2}}(N_0)\rangle = \frac{1}{\sqrt{\Omega_1}} \sum_j e^{-\frac{\alpha^2}{2}(j-N_0)^2} e^{i\frac{\pi}{2}j} |j\rangle \quad (12)$$

at $t = 0$, where Ω_1 is the normalization factor and N_0 is the initial central position of the GWP at the input chain A . The single excitation basis vector $|j\rangle = S_{A,j}^+ |d\rangle$ is defined by the polarized state $|d\rangle$ with all spins aligned down. As mentioned in the introduction, the conclusion we obtained for bosonic system is exact for the single-magnon case. It is known from the previous work [11] that such GWP can approximately propagate along a homogenous chain without spreading. Then at a certain time t , such GWP evolves into

$$|\Phi(t)\rangle = \cos \theta |\psi_{B\frac{\pi}{2}}(N_t)\rangle + \sin \theta |\psi_{C\frac{\pi}{2}}(N_t)\rangle \quad (13)$$

where $N_t = N_0 + 2tJ_A - M$, i.e., the beam splitter can split the GWP into two cloned GWPs completely.

In order to verify the above analysis, a numerical simulation is performed for a GWP with $\alpha = 0.3$ in a finite system with $N_A = N_B = N_C = 50$. Let $|\Phi(0)\rangle$ be a normalized initial state. Then the reflection factor at time t can be defined as $R(J_{nC}, J_{nB}, t) = \sum_{j \in D'} |\langle j | e^{-iHt} |\Phi(0)\rangle|^2$ to depict the reflection at the node where $D' = [1, M - 1]$. At an appropriate instant t_0 , $R(J_{nC}, J_{nB}) = R(J_{nC}, J_{nB}, t_0)$ as a function of J_{nC} and J_{nB} is plotted in Figure 2. Here J_{nC} and J_{nB} are in the unit of J_A . It shows that around the coupling matching condition (11), the reflection factor vanishes, which is just in agreement with our analytical result.

4 Dynamic of beam splitter as entangler

Now we consider how the SSSN can behave as an entangler to produce spin entanglement with the Y -beam as an illustration. Let the input state $|\phi(0)\rangle$ to be a single magnon excitation state in the leg A (e.g., $= S_{A,j}^+ |d\rangle$)

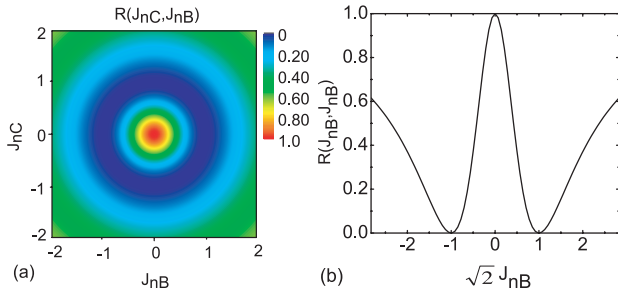


Fig. 2. (Color on line) (a) The contour map of the reflection factor $R(J_{nC}, J_{nB})$ as a function of J_{nC}, J_{nB} for the GWP with $\alpha = 0.3$ and momentum $\pi/2$ in a finite system with $N_A = N_B = N_C = 50$. It shows that around the matching condition, i.e. the circle $J_{nC}^2 + J_{nB}^2 = J_A^2$, the reflection factor approaches zero. (b) The profile of $R(J_{nC}, J_{nB})$ along $J_{nC} = J_{nB}$. J_{nC} and J_{nB} are in the unit of J_A .

or $|\psi_{A\frac{\pi}{2}}(N_0)\rangle$ introduced by Eq. (12)). It can propagate into the legs B and C through the node with some reflection. On the other hand, the spin wave can be regarded as being transferred along the virtual legs a and b . Once we manipulate the coupling constants to satisfy the coupling matching condition, the spin wave can only enter the leg a rather than b without any reflection. Then the final state is of the magnon excitation only in the leg a . As an illustration, a transferring wavepacket in the imaginary chain with the location beyond the input arm can be written as $|\phi(t)\rangle = \sum_{j=1}^N C(j, t) S_{a, M+j}^+ |d\rangle$. Here $S_{a, M+j}^+ |d\rangle = \cos\theta |u_{jB}\rangle \otimes |d_C\rangle + \sin\theta |d_B\rangle \otimes |u_{jC}\rangle$, $|u_{jF}\rangle = S_{F, j}^+ |d_F\rangle$ ($F = B, C$) represents single-magnon excitation from the fully polarized state $|d_F\rangle$ of the chain F with all spin down and $C(j, t)$ describes the shape of the wavepacket at a certain instant t . This is an entangled state and then the Y -beam acts as an entangler similar to that in quantum optical systems.

To quantitatively characterize entanglement of two separated waves $|\psi_{B, C\frac{\pi}{2}}(N_t)\rangle$ obtained by the beam splitter, the total concurrence with respect to the two wave packets located at the ends of legs B and C can be calculated as $C(t) = \sum_{i \in D} |\langle \Phi(t) | (S_{B, i}^+ S_{C, i}^- + S_{B, i}^- S_{C, i}^+) | \Phi(t) \rangle|$ according to references [18, 19]. Here, $D = [N - W, N]$, $W = 4\sqrt{\ln 2}/\alpha$ is the width of the wave packet is corresponding to the size of the wave packet. We set the range of the sum to match the local measurement for the electron in the experiment since the non-spreading wave packet is regarded as a local particle. On the other hand, the concurrence is also the function of J_{nC} and J_{nB} . Numerical simulation is performed for a GWP with $\alpha = 0.3$ and momentum $\pi/2$ in a finite system with $N_A = 50$, $N_B = 50$, and $N_C = 50$. The maximal concurrence $C_{\max}(J_{nC}, J_{nB}) = \max\{C(t)\}$ as a function of J_{nC} and J_{nB} is plotted in Figure 3. Here J_{nC} and J_{nB} are in the unit of J_A . It shows that two split wave packets yield the maximal entanglement just at the coupling matching point $J_{nC} = \pm J_{nB} = \pm J_A/\sqrt{2}$.

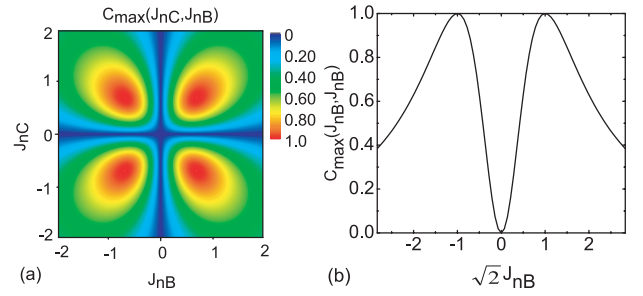


Fig. 3. (Color on line) (a) The contour map of maximal concurrence of two GWPs at two legs A and B , $C_{\max}(J_{nC}, J_{nB})$ for the same setup as that in Figure 2. It is found that two GWPs yield the maximal entanglement at the point $J_{nC} = \pm J_{nB} = \pm J_A/\sqrt{2}$. (b) The profile of $C_{\max}(J_{nC}, J_{nB})$ along $J_{nC} = J_{nB}$. J_{nC} and J_{nB} are in the unit of J_A .

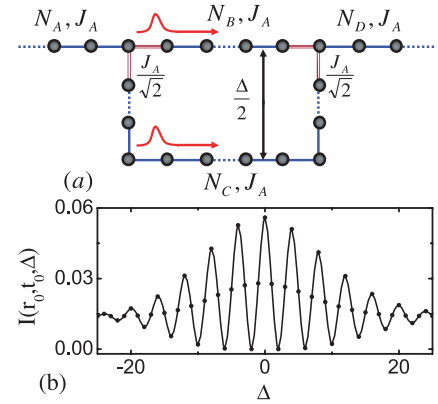


Fig. 4. (Color on line) (a) The interferometric network with an input chain A and output chain D , which consists of two Y -beams. Δ is the “optical path difference” which determines the interference pattern of output spin wave. (b) The interference pattern of output wave in the leg D ($r_0 = 50$, $t_0 = 100/J_A$) for the GWP with $\alpha = 0.3$ in the interferometric network with $N_A = N_B = N_D = 50$, $N_C = N_B + \Delta$.

5 Quantum interferometer for spin wave

Finally, we consider in detail a more complicated spin network (SN) than the Y -beam, the quantum interferometer for spin wave, which consists of two Y -beams (see Fig. 4a). Similar to the optical interferometer, where the polarization of photon is utilized to encode information, the SN uses the spin down and up to encode the quantum information.

We still use the evolution of GWP to demonstrate the physical mechanism of such setup. Firstly, we consider the simplest case with the path difference (defined in Fig. 4a) $\Delta = 0$. It is easy to show that such network is equivalent to two independent virtual chains with lengths $N_A + N_B + N_D$ and N_B respectively when the coupling matching condition is satisfied. Then the initial GWP will be transmitted into the leg D without any reflection. This fact can be understood according to the interference of two split GWPs. It means that the nonzero Δ should affect the shape of the pattern of output wave.

Actually, from the above analysis about the GWP propagating in the Y -beam, we note that the conclusion can be extended to the Y -beam consisting of two different length legs $N_B \neq N_C$. It is due to the locality of the GWP and the fact that the speed of the GWP only depends on the coupling constant. Thus the interference pattern at site r_0 and time t_0 in leg D can be presented as $I(r_0, t_0, \Delta) = |\langle r_0 | \exp(-iHt_0) |\Phi(0)\rangle|^2$. Numerical simulation of $I(r_0, t_0, \Delta)$ for the input GWP in the interferometric network with $N_A = N_B = N_D = 50$, $N_C = N_B + \Delta$ is performed. For $r_0 = 50$, $t_0 = 100/J_A$, a perfect interference phenomenon by $I(r_0, t_0, \Delta)$ is observed for the range $\Delta \in [-25, 25]$ in Figure 4b.

In summary, we point out that our coherent quantum network for spin wave can be implemented by an array of quantum dots or other artificial atoms. It will enable an elementary quantum device for scalable quantum computation, which can coherently transfer quantum information among the qubits to be integrated. The observable effects for spin wave interference may be discovered in the dynamics of magnetic domain in some artificial quantum material.

This work is supported by the NSFC with grant Nos. 90203018, 10474104 and 60433050; and by the National Fundamental Research Program of China with Nos. 2001 CB309310 and 2005 CB724508.

References

1. R. Loudon, *The quantum theory of light* (Oxford, 2000); M.O. Scully, M.S. Zubairy, *Quantum Optics* (Oxford, 1997)
2. J.D. Franson, Phys. Rev. A **56**, 1800 (1997); K. Jacobs, P.L. Knight, Phys. Rev. A **54**, R3738 (1996); T. Wang, M. Kostrun, S.F. Yelin, Phys. Rev. A **70**, 053822 (2004)
3. M. Zukowski, A. Zeilinger, M.A. Horne, Phys. Rev. A **55**, 2564 (1997); J.L. van Velsen, Phys. Rev. A **72**, 012334 (2005)
4. H. Rauch, W. Treimer, U. Bonse, Phys. Lett. A **47**, 369 (1974)
5. D. Cassetari, B. Hessmo, R. Folman, T. Maier, J. Schmiedmayer, Phys. Rev. Lett. **85**, 5483 (2000); U.V. Poulsen, K. Mømer, Phys. Rev. A **65**, 033613 (2002); D.C.E. Bortolotti, J.L. Bohn, Phys. Rev. A **69**, 033607 (2004)
6. F. Burgbacher, J. Audretsch, Phys. Rev. A **60**, R3385 (1999); N.M. Bogoliubov, A.G. Izergin, N.A. Kitanine, A.G. Pronko, J. Timonen, Phys. Rev. Lett. **86**, 4439 (2001)
7. S. Bose, Phys. Rev. Lett. **91**, 207901 (2003); M.-H. Yung, S. Bose, Phys. Rev. A **71**, 032310 (2005)
8. M. Christandl, N. Datta, A. Ekert, A.J. Landahl, Phys. Rev. Lett. **92**, 187902 (2004); C. Albanese, M. Christandl, N. Datta, A. Ekert, Phys. Rev. Lett. **93**, 230502 (2004)
9. Y. Li, T. Shi, B. Chen, Z. Song, C.P. Sun, Phys. Rev. A **71**, 022301 (2005); Z. Song, C.P. Sun, Low Temperature Physics **31**, 686 (2005)
10. T. Shi, Y. Li, Z. Song, C.P. Sun, Phys. Rev. A **71**, 032309 (2005); Y. Li, Z. Song, C.P. Sun, e-print [arXiv:quant-ph/0504175](https://arxiv.org/abs/quant-ph/0504175)
11. S. Yang, Z. Song, C.P. Sun, Phys. Rev. A **73**, 022317 (2006)
12. M.B. Plenio, J. Hartley, J. Eisert, New J. Phys. **6**, 36 (2004); A. Perales, M.B. Plenio, J. Opt. B **7**, S601–S609 (2005)
13. A. Kay, M. Ericsson, New J. Phys. **7**, 143 (2005)
14. G.D. Chiara, R. Fazio, C. Macchiavello, S. Montangero, G.M. Palma, Phys. Rev. A **70**, 062308 (2004); G.D. Chiara, R. Fazio, C. Macchiavello, S. Montangero, G.M. Palma, Phys. Rev. A **72**, 012328 (2005)
15. Q. Chen, J. Cheng, K.-L. Wang, J. Du, e-print [arXiv:quant-ph/0510147](https://arxiv.org/abs/quant-ph/0510147)
16. A.M. Childs, R. Cleve, E. Deotto, E. Farhi, S. Gutmann, D.A. Spielman, e-print [arXiv:quant-ph/0209131](https://arxiv.org/abs/quant-ph/0209131)
17. T. Holstein, H. Primakoff, Phys. Rev. **58**, 1098 (1940)
18. X. Wang, P. Zanardi, Phys. Lett. A **301**, 1 (2002); X. Wang, Phys. Rev. A **66**, 034302 (2002)
19. X.-F. Qian, Y. Li, Y. Li, Z. Song, C.P. Sun, Phys. Rev. A **72**, 062329 (2005)